MRS Communications (2017), 7, 755–769
© Materials Research Society, 2017
doi:10.1557/mrc.2017.100

MRS Communications

Prospective Article

High-frequency organic rectifiers through interface engineering

Chan-mo Kang, IoT Research Division, Electronics and Telecommunications Research Institute, Daejeon 34129, Korea
Hyeonwoo Shin, and **Changhee Lee,** Department of Electrical and Computer Engineering and Inter-university Semiconductor Research Center, Seoul National University, 08826, Korea

Address all correspondence to C. Lee at **chlee7@snu.ac.kr**

(Received 12 June 2017; accepted 8 September 2017)

Abstract

The demand for high-frequency (HF) and low-cost rectifiers has encouraged many researchers to investigate organic rectifiers. Recently, organic rectifiers with enhanced intrinsic carrier mobility and charge injection efficiency have enabled operating frequencies to reach up to a gigahertz (GHz). The metal/organic and organic/organic interfaces have played a significant role in determining the electrical properties of the organic rectifiers. In this prospective article, we review the structure of organic rectifiers and present the current state-of-the-art to attain their HF performance. We discuss methods for improving their electrical properties using interface engineering and present future prospects for practical use of GHz-operable organic rectifiers.

Introduction

During the last decade, organic semiconductors have gained considerable attention as an active layer for next-generation electronics due to ease in their patterning and their tunable molecular structure, flexibility, light-weight, and large-area applicability.[1–4] In particular, their promising potential low-cost is expected to begin an era of disposable electronics.[5,6] Organic radio-frequency identification (RFID) tags, which can be used to detect objects automatically in the near-field region (<10 m), are one of the emerging applications in disposable electronics. For this reason, organic RFID tags have been extensively studied over the past few decades.[7–11]

To realize organic RFID tags at the standard frequency of 13.56 MHz for high-frequency (HF) systems and 860–960 MHz for ultra-high-frequency (UHF) systems, organic rectifiers that convert radio frequency (RF) signal to DC power for operating circuits in the tags should be properly operated at the given frequency. Figure 1 and Table I summarize previously published characteristics of organic rectifiers, including the 3 dB frequency, at which the output voltage drops to half. Although different types of organic rectifiers have been proposed, the organic rectifiers with a vertical Schottky diode structure have been the most commonly reported devices because of their structural advantages in frequency characteristics. Most of the organic rectifiers have been HF systems due to the limited charge-transport properties and, hence, the operating frequencies of RFID tags have mainly been distributed around 13.56 MHz.[9–11] The HF RFID systems use inductive coupling for communication between a reader and a tag that can be operated only in the near field (<1 m). To achieve longer operating distances, the operating frequency should be increased to the UHF region where the RFID systems can communicate using backscattering modulation. However, conceiving UHF RFID tags still remains a challenge due to the difficulty in fabricating ultrafast organic rectifiers, whose operating frequencies scale with their charge-transport properties. These are largely affected by metal/organic and organic/organic interface properties in the organic rectifiers. By modifying the interface properties of the organic rectifiers through interface engineering, organic rectifiers operating in the UHF region can be achieved.[12,13]

In organic devices, the interface is one of the most important factors determining their electrical properties. For example, formation of an injection barrier at metal/organic interfaces can hinder charge injection. Even if the work function of a metal electrode is matched with the highest occupied molecular orbital (HOMO) or the lowest unoccupied molecular orbital (LUMO) level of the organic semiconductor, an adversely aligned interfacial dipole can shift the vacuum level to an undesirable direction and introduce an additional energy barrier, limiting charge injection.[55–57] To overcome this issue, modifying the interfacial dipole or the insertion of a carrier injection layer can be employed.[12,14,18] The current density and rectification ratio (RR) of the organic diodes can also be designed by controlling the built-in potential formed at the metal/organic or organic/organic interfaces.[13,58–60] Moreover, the molecular orientation and alignment that determine the carrier mobility are much affected by the surface property of the underlying layer, which can be modified via interface engineering.[12,61] Because of its importance, studies on interface engineering of organic rectifiers, summarized in Fig. 2, have been intensively conducted.

https://doi.org/10.1557/mrc.2017.100 Published online by Cambridge University Press

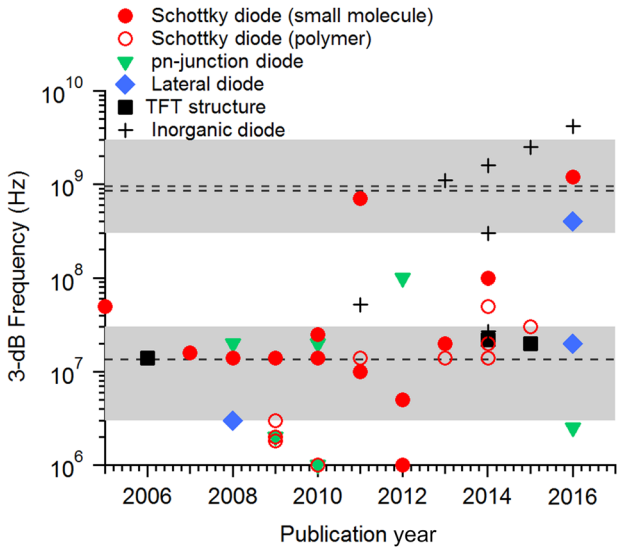


Figure 1. Frequency characteristics of organic rectifiers published over time. The gray shades indicate the range of the HF and UHF bands and the dashed lines denote the standard frequencies.

In this paper, we summarize the state-of-the-art of organic rectifiers, especially focusing on the interface engineering. First, background knowledge of the organic diode and structural advantages and disadvantages of organic rectifiers are discussed. Then, key factors that influence the frequency performance of the organic rectifiers are described. Next, interface engineering for HF organic rectifiers is reviewed in detail. Finally, a summary and prospects for the realization of HF organic rectifiers are presented. In this paper, we focus on interface engineering for the vertical diode structure, as a large number of interface studies on TFT structures have already been reported[61–63] and the vertical diode structure is mainstream in organic rectifiers.

Basic background of organic rectifiers

Metal/organic interfaces

A standard model for a metal/semiconductor junction is well established in solid-state physics. When the metal/semiconductor junction is formed, the free charge carriers in the semiconductors transfer to align the Fermi level (EF) of the semiconductor with the work function (WF) of the metal, generally resulting in energy band bending. If the WF is smaller than the EF of the p-type semiconductor, electrons in the metal are transferred to the semiconductor, forming a Schottky barrier (Φ_B), as shown in Fig. 3(a). This is called a Schottky contact. Whereas, if the WF is larger than the EF of the p-type semiconductor, it forms an ohmic contact, where the energy barrier can be neglected [Fig. 3(b)]. The above model is well suited for inorganic semiconductors, but in the case of organic semiconductors, this model needs to be modified, as the organic semiconductors have a large band gap (2–3 eV) and a small number of free charge carriers are thermally excited. Thus, energy band bending for the organic semiconductor is generally negligible. More importantly, the organic semiconductor interacts with adjacent materials, forming an interfacial dipole as shown in Fig. 3(c).[57,64] In addition, a large number of interfacial states could result in Fermi-level pinning, such that the energy barrier at the organic/metal interface is pinned irrespective of WF. This dipole-induced energy level shift and Fermi-level pinning make the energy barrier at organic/metal interface unpredictable, and significantly affects the charge-transport properties of the organic devices. Therefore, proper modification of metal/organic interface properties is inevitable to achieve the HF organic rectifiers.

Charge transport in organic diodes

When the Schottky barrier is formed in the metal/organic interface and the current is limited by the injection of charges rather than the bulk of the semiconductors, the current conduction mechanism is generally governed by a thermionic emission model. This model is based on the assumption that hot carriers, which have kinetic energy larger than the barrier height, can go across the barrier and contribute to charge conduction. The current of the thermionic emission model can be expressed as Eq. (1)[65,66]

$$I = I_S\left(\exp\frac{eV}{k_B T} - 1\right), \tag{1}$$

where the I_S is the saturation current, e is the elementary charge, V is the applied voltage, k_B is the Boltzmann constant, and T is the temperature. I_S is expressed in Eq. (2) as:[65,66]

$$I_S = AA^*T^2\exp\left(-\frac{\Phi_B}{k_B T}\right), \quad A^* = \frac{4\pi k_B^2 m^*}{h^3}, \tag{2}$$

where A is the area of the diodes, A^* is the Richardson constant, Φ_B is the Schottky barrier height, m^* is the effective mass, and h is the Planck constant.

If the injection barrier in the metal/organic interface is small or negligible, then the metal/organic interface forms an ohmic contact and the current is limited by the bulk of the organic semiconductors rather than the metal/organic interface. At low voltages, whole charges in the bulk of the organic layer are ejected through the counterpart metal electrode; therefore, there will be no charge distribution in the organic semiconductor. In this case, the carrier transport follows Ohm's law, where the current is linearly dependent on the voltage. As the voltage increases, a greater number of charge carriers are injected before it is fully ejected, so a space charge is created. These phenomena lead to a current that is called the space-charge limited current (SCLC), which, in the case of semiconductors or insulating materials, generally follows Mott–Gurney law.[67]

$$J = \frac{9}{8}\varepsilon_0\varepsilon_r\mu\frac{V^2}{d^3}, \tag{3}$$

https://doi.org/10.1557/mrc.2017.100 Published online by Cambridge University Press

Table I. Summary of previously published characteristics of organic rectifiers. For comparison, recent progress of thin film or printable inorganic rectifier is included.

Publication year	Type	Structure	RR	$J@V$ (A/cm^2@V)	3 dB frequency (MHz)	Ref.
2005	SCH-S	Au/PEDOT:PSS/pentacene/Al	20	1500@5	>50	[14]
2007	SCH-S	Al/CuPc/Au	6000	29.3@3	>13.56	[15]
2008	SCH-S	Au/pentacene/Al	3000	2.88@3	>13.56	[16]
2009	SCH-S	Au/pentacene/Al	–	–	>13.56	[11]
2010	SCH-S	Cu/CuTCNQ/pentacene/Al	2×10^6	0.51@5	>13.56	[17]
2010	SCH-S	Au/MoO_3/pentacene/Al	1000	1@3	>25	[18]
2011	SCH-S	Al/WO_3/HMDS/C_{60}/BCP/Al	4.6×10^4	46.5@1	700	[13]
2011	SCH-S	Al/pentacene/MoO_3/Au	1000	0.2@3	10	[19]
2012	SCH-S	Al/pentacene/Au	3×10^4	0.1@5	1	[20]
2012	SCH-S	Al/pentacene/Au	2×10^5	100@10	5	[21]
2013	SCH-S	Al/CuPc/Au	8.3×10^6	2.5@5	20	[22]
2014	SCH-S	Au/MoO_3/pentacene/Al	5.7×10^5	2.9@3	>100	[23]
2016	SCH-S	Au/PFBT/pentacene/Al	1.1×10^7	100@3	1240	[12]
2009	SCH-P	Ag/P3HT/Al	2900	0.1@5	1.8	[24]
2009	SCH-P	Cu/PTAA/Ag	3.3×10^4	0.002@5	3	[25]
2009	SCH-P	Au/PEDOT:PSS/P3HT/Al	3×10^4	0.1@3	>2	[26]
2010	SCH-P	Ni/Au/P3HT/Al	393	12.54@5	1	[27]
2011	SCH-P	InZnO/PEDOT:PSS/PQT-12/Al	2×10^4	6@5	>14	[28]
2013	SCH-P	Cu/PTAA/Ag	–	–	13.56	[29]
2014	SCH-P	Cu/PTAA/Ag	–	–	20	[30]
2014	SCH-P	ITO/PEDOT:PSS/TFB/Al	–	0.2@4	>50	[31]
2014	SCH-P	Al/AlO_x/FS102/PEDOT:PSS/Au	10^4	100@3	0.02	[32]
2014	SCH-P	Cu/PTAA/Ag	100	0.02@4	13.56	[33]
2015	SCH-P	Cu/PTAA/Ag	100	0.04@5	30	[34]
2016	SCH-L	Au/C_{60}:polystyrene/Al	2000	2×10^{-7}A@2	400	[35]
2008	PN-H	ITO/ZnO/pentacene/Au	3000	160@5	>20	[36]
2009	PN-H	ITO/ZnO/PQT-12/Au	400	400@2.5	2	[37]
2010	PN-H	ITO/ZnO/pentacene/Au	10^4	1.5@2.5	>1	[38]
2010	PN-H	ITO/ZnO/PEDOT:PSS/Au	330	0.01A@4	20	[39]
2012	PN	Al/p-pentacene/pentacene/n-C60/Al	3.3×10^4	0.2@1	100	[40]
2016	PN	ITO/TPD/C_{60}/Al	10^4	0.55@3	2.5	[41]
2008	SSD	Au/PQT-12/Au	1.5	10^{-6}A@80	3	[42]
2016	SSD	Au/PQT-12/Au	2.86	2×10^{-8}A@10	20	[43]

Continued

https://doi.org/10.1557/mrc.2017.100 Published online by Cambridge University Press

Table I. Continued

Publication year	Type	Structure	RR	$J@V$ (A/cm^2@V)	3 dB frequency (MHz)	Ref.
2006	TFT	TiW/SiO_2/Au/pentacene	100	10^{-8}A@10	>14	[44]
2011	TFT	Al/PVP/pentacene/Al	10^4	7×10^{-5}A@40	>0.001	[45]
2014	TFT	Cr/Au/Cr/Al_2O_3/C10-DNBDT/Au	10^9	1.5×10^{-3}A@20	22	[46]
2015	TFT	Al/parylene/DNTT/Au	5×10^7	10^{-3}A@10	20	[47]
2012	VOT	Al/Au/C_{60}/Al/C_{60}/C_{60}:W_2(hpp)$_4$/Au/Al	2900	1@2	0.1	[48]
2013	SCH-I	Ti/Pd/InGaZnO/Mo	10^8	300@1	1100	[49]
2014	SCH-I	Al/Si/$NbSi_2$/Carbon/Ag	19	1.9×10^{-5}A@2	1600	[50]
2015	SCH-I	Pt/InGaZnO/Al	450	150@0.8	2450	[51]
2016	SCH-I	Pt/InGaZnO/Al	2.2×10^4	0.65@1	4200	[52]
2014	PN-I	ITO/InGaZnO/Cu_2O/Pt	10^4	0.1@0.6	>27	[53]
2011	SSD-I	Al/ZnO/Al	2.56	2.3×10^{-5}A@10	>51.5	[54]
2014	TFT-I	gate/Al_2O_3/In_2O_3/Ti/Au	10^5	5×10^{-3}A@8	300	[7]

SCH-S: Schottky diodes based on small molecules; SCH-P: Schottky diodes based on polymers; SCH-L: lateral Schottky diodes; PN-H: organic/inorganic hybrid pn-junction diodes; PN: organic pn-junction diodes; SSD: organic self-switching devices; TFT: organic TFTs with diode connection; VOT: vertical organic transistors with diode connection; SCH-I: inorganic Schottky diodes; PN-I: inorganic pn-junction diodes; SSD-I: inorganic self-switching devices; TFT-I: inorganic TFTs with diode connection; BCP: 2,9-dimethyl-4,7-diphenyl-1,10-phenanthroline; TFB: poly(fluorene-alt-triarylamine); FS102: amorphous co-polymer of arylamine and a fused aromatic species (Flexink Ltd., U.K.); p-pentacene: 2,2-(perfluoronaphthalene-2,6-diylidene) dimalononitrile doped pentacene; W_2(hpp)$_4$: tetra-kis(1,3,4,6,7,8-hexahydro-2H-pyrimido[1,2-a]pyrimidinato) ditungsten(II); n-C_{60}: W_2(hpp)$_4$ doped C_{60}; TPD: N,N′-bis (3-methylphenyl)-N,N′-diphenylbenzidine; PVP: poly 4-vinylphenol; C10-DNBDT: 3,11-didecyldinaphtho[2,3-d:2′,3′-d′]benzo[1,2-b:4,5-b′]dithiophene; DNTT: Dinaphtho[2,3-b:2′,3′-f]thieno[3,2-b]thiophene.

where ε_0 is the vacuum permittivity, ε_r is the relative permittivity, μ is the carrier mobility of the organic semiconductor, and d is the thickness of the organic semiconductor. However, the actual current mechanism of the organic semiconductor is more complex because of the presence of trap states. Assuming that the traps are exponentially distributed, the current can be expressed as follows:[67]

$$J \approx e^{1-m}\mu N_C\left(\frac{2m+1}{m+1}\right)^{m+1}\left(\frac{m}{m+1}\frac{\varepsilon_0\varepsilon_r}{N_t}\right)^m\frac{V^{m+1}}{d^{2m+1}},$$
$$m=\frac{T_t}{T}, \quad (4)$$

where N_C is the effective density of conduction band states, N_t is the trap density, and T_t is the temperature parameter characterizing the trap distribution. When an electric field is applied, furthermore, and all of the trapping sites are filled in the organic semiconductor, the SCLC becomes independent of traps, and the equation can be simply expressed as Eq. (3).

The SCLC can be applicable when the current is dominated by drift. For organic diodes, the work function difference between the anode and cathode creates built-in potential. When the applied voltage is much higher than the built-in voltage, the current obeys the Mott–Gurney law. However, when the applied voltage is smaller than the built-in voltage, the internal electric field in the organic is negative, leading to a negative drift current. Different barrier heights at the anode and cathode contacts yield a distribution of hole density (electron density, in the case of an n-type organic material), allowing a positive diffusion current to flow. At the low-voltage region, the positive net current indicates that the dominant current mechanism is diffusion, which can be expressed as follows:[68]

$$J=\frac{e\mu N_C(\Phi_B-b-V)[\exp(eV/k_BT)-1]}{d\exp(eb/k_BT)[\exp\{e(\Phi_B-b)/k_BT\}-exp(eV/k_BT)]},$$
$$b=\frac{k_BT}{e}\left[\ln\left(\frac{e^2N_Cd^2}{2k_BT\varepsilon_0\varepsilon_r}\right)-2\right], \quad (5)$$

where b is the band-bending parameter. For organic diodes, therefore, the current exponentially increases in the low-voltage region [Eq. (5)] and quadratically increases in the high-voltage region [Eq. (3)] with regard to the applied voltage.

Structure of organic rectifiers

A rectifier consists of a capacitor and a rectifying diode. When a forward bias is applied to the rectifier, charges flow through the

https://doi.org/10.1557/mrc.2017.100 Published online by Cambridge University Press

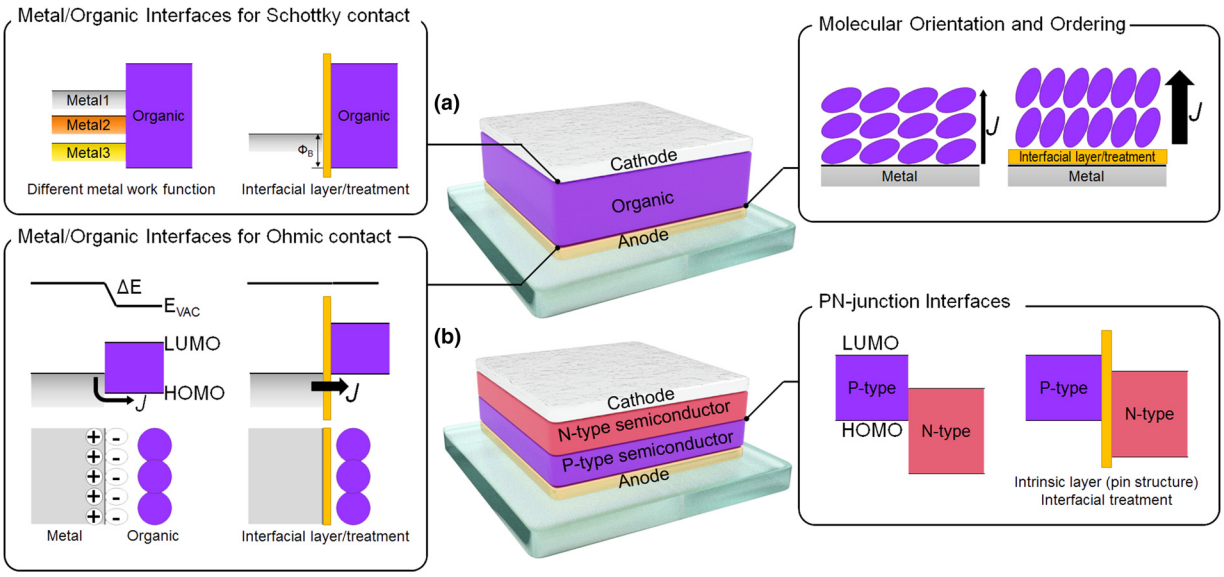


Figure 2. Summary of interface engineering for organic rectifiers, where Φ_B is the Schottky barrier height and J is the current density. (a) Structures of the Schottky diode and (b) pn-junction diode.

rectifier and are stored at the capacitor, but the stored charges do not discharge by the reverse bias because the diode conducts only when it is forward-biased. Several device structures and electrical circuits have been proposed to give the devices the properties of a rectifier and to improve their electrical properties.

A Schottky diode [Fig. 2(a)] is a metal/semiconductor/metal structure with a Schottky contact at the metal/semiconductor interface and is the most commonly used structure in organic rectifiers.[11–30,33,34] The built-in potential at the Schottky contact is effectively reduced by a forward bias, which allows high current to flow that is limited by the Schottky barrier when the reverse bias is applied. The metal/organic contact at the counter electrode should be ohmic to achieve a high forward current. A Schottky diode in a vertically sandwiched structure is relatively easy to fabricate and it is facile to control the thickness of the organic layer and the device area. For these reasons, it has been the main rectifier structure adopted by many researchers. A laterally co-planar structure is tolerant of the pinholes and defects of the organic layer, which can cause high leakage current and breakdown in a vertically sandwiched structure. However, difficulty in achieving a uniform sub-micrometer gap of two different electrodes is a disadvantage of the laterally co-planar structure of the Schottky diode. Semple et al. reported a 20 nm gap co-planar diode based on solution-processed C_{60}:polystyrene by using adhesion-lithography.[35] Because of this short gap, an estimated 3 dB frequency of 400 MHz was accomplished.

The Schottky diode is advantageous in terms of achieving high operating frequencies due to its relatively small capacitance.[12–14] However, the relatively high leakage current of the Schottky diode can be an issue, especially at high temperature. Because the leakage current of the Schottky diode is primarily limited by thermionic injection, it could be exponentially increased as the temperature is increased.

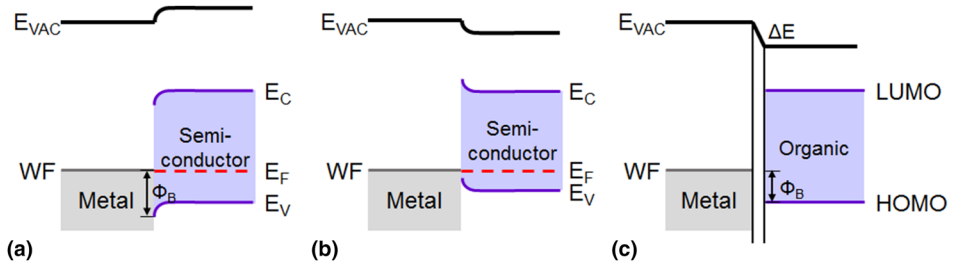


Figure 3. Energy level alignment at the metal/semiconductor contact for (a) the Schottky contact, (b) ohmic contact, and (c) contact with an organic semiconductor.

https://doi.org/10.1557/mrc.2017.100 Published online by Cambridge University Press

A pn-junction diode consists of n- and p-type semiconductors sandwiched between two metal electrodes [Fig. 2(b)]. A pn-junction at the interface of the p- and n-type semiconductors generates the built-in potential, which can be decreased by a forward bias and increased by a reverse bias. Because the pn-junction has the rectification property, the metal/organic contact in the anode and the cathode should be ohmic. The advantage of the pn-junction diode is that the current can be easily controlled by adjusting the doping concentration or the thickness of semiconductor layer or by inserting an intrinsic layer.[40,69] Also, high doping concentration at the metal/organic interface guarantees a quasi-ohmic contact, enabling free choice of metal electrodes. Moreover, the pn-junction diode exhibits a small leakage current compared with the Schottky diode. The major disadvantage of the pn-junction diode is its relatively low-frequency performance due to the presence of the pn-junction capacitance. The lack of high mobility n-type organic materials is another obstacle to further improvements. Thus, p-organic/n-inorganic hybrid diodes have also been studied.[36–39]

Key factors of organic rectifiers to achieve high-frequency performance

The frequency performance of organic rectifiers scale with the charge transport properties of the organic diodes and there are key factors determining these properties. To increase the forward current of an organic diode, high injection efficiency and mobility are required. In addition, the rectifying barrier height affects the forward current as well as the reverse current. The thickness of the semiconductor layer is directly related to the transit time of the device, which determines the frequency response of the rectifier. The device area is not directly related to the frequency response, but it is also an important factor. These factors will be discussed in more detail below.

Barrier height and mobility

To reduce the injection barrier height for achieving high injection efficiency, several methods have been studied such as energy level alignment using high work function metals or alloys,[70] thermal and electrical annealing, reducing the interface dipole via a self-assembled monolayer (SAM),[12,71–73] and inserting a charge injection layer such as a conducting polymer,[14,28,74,75] a doped organic layer,[76,77] an organic material having an intermediate energy level,[78] or a transition metal oxide.[79] The mobility is principally determined by the intrinsic molecular structure, but it is also much affected by molecular orientation and alignment. To enhance molecular orientation and alignment, controlling the surface energy through interface engineering has been studied.[12,80,81] The rectifying barrier height is also one of the important factors determining diode characteristics. If the forward current is limited by bulk characteristics due to low mobility, the reverse current can effectively be suppressed by increasing the barrier height.[59] If the forward current is limited by the contact, it can be enhanced by lowering the barrier height.[13] The aforementioned factors can be controlled by interface engineering, which will be elaborated later.

Semiconductor layer thickness

Generally, organic semiconductors operate in the SCLC regime and obey the Mott–Gurney law given by Eq. (3). If the current of the organic diode follows the Mott–Gurney law and ignoring the leakage current, the frequency performance of the organic rectifier can be expressed by[14]

$$f_{MAX} = \frac{9\mu}{16\pi d^2 V_o}\left[(-3V_o + V_F)\sqrt{V_{IN}^2 - (V_o + V_F)^2} + (V_{IN}^2 + 2V_o^2)\arccos\left(\frac{V_o + V_F}{V_{IN}}\right)\right], \quad (6)$$

where f_{MAX} is the maximum frequency, V_O is the output voltage, V_F is the transition voltage where the conduction mechanism changes from ohmic to SCLC, and V_{IN} is the peak input voltage applied to the rectifier. From Eq. (6), the frequency response is inversely proportional to the square of the thickness. Thus, if the organic diode follows the SCLC mechanism, a thin organic layer is beneficial for the frequency performance, which is also consistent with a transit time-based equation.[31] A large number of studies have been conducted to elucidate the effect of the thickness of the rectifiers.[18,25–27,31,34] For solution processed organic rectifiers, where the current dominantly obeys Eq. (3) due to the low mobility (<0.01 cm^2/V/s), the frequency performance increases as the thickness increases.[25–27,31,34] For some organic materials whose current is no longer dominantly restricted by a space-charge limited mechanism, the relationship between the frequency performance and the thickness may be different. From the relationship between Eqs. (3) and (6), it can be speculated that f_{MAX} increases as d decreases when the exponent of d in Eq. (3) is larger than 1.[18] In other words, the frequency performance is better when the value of the product $J \times d$ is higher. Figures 4(a) and 4(b) show measured current densities of pentacene diodes with thicknesses of 56 and 104 nm, respectively. The solid lines indicate linearly scaled current densities using $J(V) = 84/56 \times J_{84\,nm}(V)$ or $J(V) = 84/104 \times J_{84\,nm}(V)$, respectively, where $J_{84\,nm}(V)$ is the current density as a function of voltage for a diode thickness of 84 nm. Both measured current densities are under the solid lines, implying that the frequency performances are worse than that with a thickness of 84 nm, which is confirmed by the measured frequency performance as shown in Fig. 4(c). Meanwhile, a thin organic layer shows high leakage current and even breakdown due to high roughness, pinholes, and defects, thereby causing problems related to uniformity, yield, stability, and reproducibility.[18,34] In addition, the thin organic layer decreases the reverse breakdown voltage. For example, the reverse breakdown voltages of pentacene diodes with thicknesses of 28, 56, 84, and 104 nm were reported to be 5, 14.2, 21.3, and 24 V, respectively.[18] Ideally, the maximum reverse bias applied to the organic rectifier is twice the peak input voltage. Thus, the reverse

https://doi.org/10.1557/mrc.2017.100 Published online by Cambridge University Press

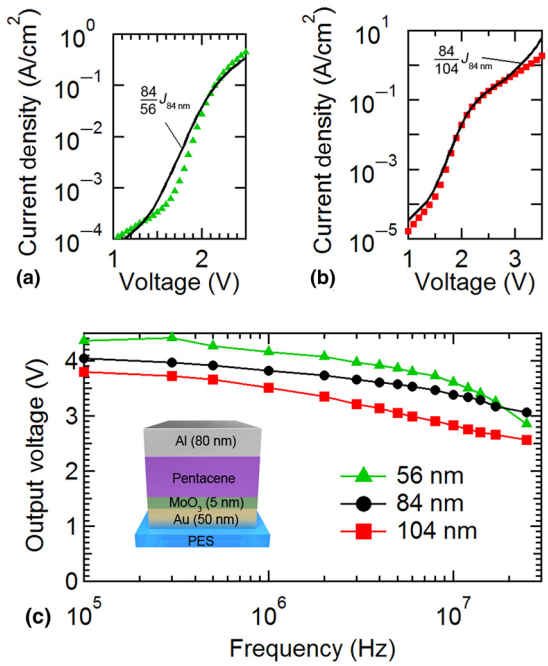


Figure 4. (a, b) *J–V* curves for pentacene diodes with thicknesses of 56 and 104 nm, respectively. The solid line indicates the linearly scaled current density of the 84 nm-thick pentacene diode. (c) Frequency responses of pentacene rectifiers of different thicknesses. The inset depicts the structure of the pentacene diode.

breakdown voltage of the organic diode should be high enough to ensure the maximum strength of an input signal at a given frequency. In summary, the frequency performance of the organic rectifier is better when the $J \times d$ value is higher, while the stability of the organic rectifier is better when the organic layer is thick. Therefore, the thickness of the organic layer should be carefully designed considering performance requirements.

Area of the organic diode

The frequency performance of an organic rectifier does not seem to be correlated with the area of the organic diode, which is absent in Eq. (6), but the effect of the area on the electrical properties should not be disregarded. A large diode area increases the conductance of the diode and power capacity, leading to the high output voltage and power transmission.[24,30] However, the corresponding load capacitance should be kept much larger than the diode capacitance to minimize the output ripple voltage. Thus, an enlarged load capacitance owing to a large diode area increases the total area of RFID tags, which reduces price competitiveness. Furthermore, large-area diodes cannot sustain the high input voltage due to worst heat dissipation, especially on the plastic substrates having low thermal conductivity.[24] Hence, small-area diodes are more stable than the large-area diodes against high RF power. For these reasons, the diode area should be carefully chosen considering the input power and the power consumption of the circuits.

Interface engineering for high-frequency organic rectifiers

The electrical properties of organic rectifiers can be controlled via interface engineering. By controlling the interfacial barrier and the surface energy, the forward and reverse current levels and the molecular orientation can be adjusted.

Improving injection efficiency

Charge injection is one of the primary factors determining the performance of organic rectifiers and improving the efficiency of charge injection can help achieve HF organic rectifiers. Generally, the surface electronic cloud of metals is rearranged by a repulsion force of the organic electronic cloud that generates a dipole at the metal/organic interface, leading to a negative vacuum level shift.[57] As for p-type organic semiconductors, the injection barrier induced by this adversely aligned dipole limits charge injection, even if the work function of the metal and the HOMO level of the organic layer are well matched. In the case of n-type organic semiconductors, the dipole effect could be beneficial. However, if the low work function of the metal matches the LUMO level of the n-type organic semiconductor, it generally becomes vulnerable to oxygen and moisture.

Inserting a charge injection layer is a commonly used method to improve charge injection efficiency. The dipole at an organic/organic interface is relatively smaller than the dipole at an organic/metal interface and, thus, employing an additional organic layer could be an effective way to reduce the injection barrier at metal/organic interfaces. One of the most widely used conducting polymers exhibiting a high work function and high conductivity is poly(3,4-ethylenedioxythiophene) : poly(styrenesulfonate) (PEDOT : PSS). The high carrier concentration of PEDOT : PSS allows to form a quasi-ohmic contact at the metal/organic interface and its high work function facilitates efficient hole injection from the PEDOT : PSS to the organic layer.[14,23,28,73] In the same manner, a doped organic layer can also be used as the hole and electron injection layer.[40,69] These conductive organic layers effectively improve charge injection, but they could give rise to a lateral leakage current, resulting in a low RR.[28] Another choice for the inter-layer is a so-called charge extraction layer that exhibits deep-lying HOMO and LUMO levels and can be created using materials such as copper hexadecafluorophthalocyanine (F16CuPc), 1,4,5,8,9,11-hexaazatriphenylenehex acarbonitrile (HAT-CN), 2,3,5,6-tetrafluoro-7,7,8,8-tetracyanoquinodimethane (F4-TCNQ), or transition metal oxides. Because charge extraction layers generally have a relatively large electron affinity value, the LUMO of the charge extraction layer is matched with the HOMO of the organic layer. Thus, holes are injected by transferring electrons from the organic layer to the charge extraction layer.[82] By employing the charge extraction layer, the current density of the pentacene diode was measured to be 2.9 A/cm^2 at 3 V, which is orders of magnitude higher than that of the diode

https://doi.org/10.1557/mrc.2017.100 Published online by Cambridge University Press

without the charge extraction layer (0.00057 A/cm^2) [Fig. 5(a)]. As a result, the 3 dB frequency reached values of more than 100 MHz for the organic rectifier with the charge extraction layer [Fig. 5(b)].

Another way to reduce the unfavorable dipole and improve hole injection is the surface treatment on the electrode. Ultraviolet ozone or plasma treatments increase OH– or O_2– groups at the surface of the electrode and lead to an increment of the effective work function.[83,84] Chemically modified electrodes such as the Copper tetracyanoquinodimethane (CuTCNQ)-modified Cu electrode increased the effective work function from 4.6 to 5.2 eV. As a result, the forward current density of the pentacene diode with the CuTCNQ-modified Cu electrode was comparable with that with an Au electrode.[17] The effective work function can also be tuned by the SAM treatment by means of the permanent dipole moment of chemisorbed SAM molecules. Perfluorinated thiol derivatives are commonly used to increase the effective work function of metals because the thiol groups strongly react with metals and fluorine atoms, exhibiting high electronegativity and forming a negative dipole moment. For example, a 1H,1H,2H,2H-perfluorodecanethiol-modified Ag electrode exhibits a negative dipole moment of −1.69 D, resulting in an increased effective work function of 0.85 eV and a reduction in the hole injection barrier by 0.5 eV.[71,72] In addition, a 2,3,4,5,6-pentafluorothiopehnol (PFBT) modified Au electrode effectively reduced the injection barrier to 0.1 eV.[85] To improve electron injection, a thin polymer (1–10 nm) surface modifier with aliphatic amine groups such as polyethylenimine ethoxylated (PEIE) and polyethylenimine (PEI) is suitable for the air-stable electron injection layer [Fig. 6(a)]. Due to the strong molecular and interface dipole of PEIE and PEI, the effective work function of the target material can be lowered by up to 1.5 eV [Fig. 6(b)].[86] As a result, insertion of a 10 nm-thick PEIE layer at an indium tin oxide(ITO)/copper(II) phthalocyanine (CuPc) interface greatly reduces the electron injection barrier from 1.3 to 0.36 eV [Figs. 6(c) and 6(d)]. This concept of the work function shifting method can also be applied to form a rectifying contact for p-type organic materials.[80]

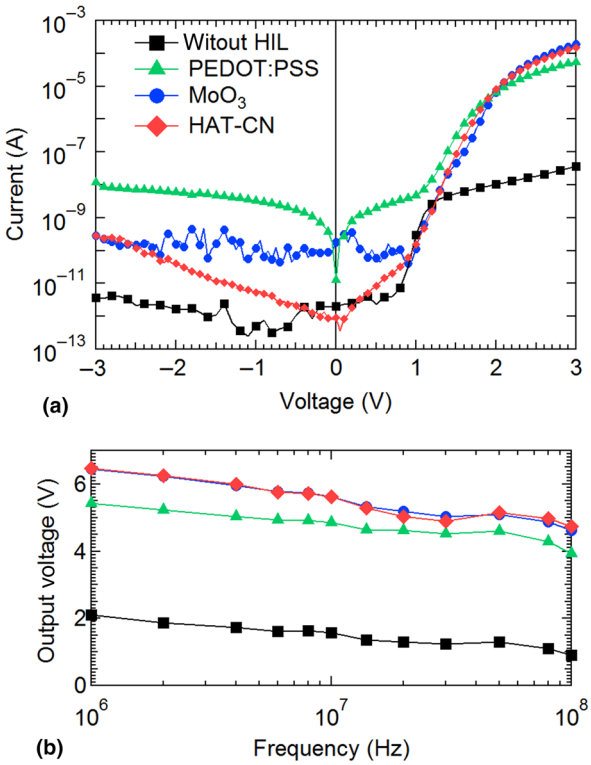


Figure 5. (a) *J–V* and (b) frequency characteristics of the organic rectifiers with various hole injection layers (HILs).

Improving molecular orientation and crystalline order

The molecular orientation and packing structure of the organic semiconductor are much affected by surface properties of the underlying layer. High packing density and long-range crystalline order are advantageous to achieve high mobility, which is favorable for the fabrication of HF organic rectifiers. Studies have shown that pentacene molecules on bare gold and SAM-modified gold exhibit different microstructures.[12,87,88] For instance, Raman spectra of pentacene films on gold and PFBT-modified gold show distinctive intensity differences at 1598 cm^{-1} [Fig 7(a)]. Since the Raman peak at 1598 cm^{-1} indicates the long-axis vibration mode of pentacene, it is direct evidence of the molecular orientation change of pentacene within the PFBT-modified gold surface. In addition, the x-ray diffraction (XRD) patterns show *c*-axis oriented peaks of (001) and (002) planes for pentacene on PFBT-modified gold and relatively weak *ab*-axis oriented peaks of (110), (022), and (−201) planes for pentacene on bare gold [Fig. 7(b)]. These indicate that the pentacene molecules are likely to stand up on PFBT-modified gold and lie down on bare gold. Even if the grain sizes of pentacene on PFBT-modified gold and bare gold are the same, the charge carriers have less chance to encounter grain boundaries in a vertical direction for the pentacene film with standing up geometry, leading to an increase in mobility. The pentacene film on bare Au exhibits randomly oriented grains with the crystalline disorder. However, the pentacene film on PFBT-modified Au shows more uniform grain sizes and thicknesses [Fig. 7(c)]. Thus, the vertical mobility of the pentacene film on PFBT-modified Au is increased from 6.8×10^{-4} to 1.1×10^{-1} cm^2/V/s. In addition, the PFBT-modified Au electrode also effectively reduces the injection barrier as mentioned earlier, enabling diodes to reach a high-current density of 100 A/cm^2 at 3 V. Owing to such a mobility improvement and the high-charge injection efficiency, a 3-dB frequency of 1.24 GHz was achieved for the pentacene rectifier with PFBT-modified Au [Fig. 7(d)]. Another interesting study reported that the performances of Au/PEIE/CuPc/Au and Au/CuPc/PEIE/Au organic diodes, which have the same structures but with different deposition order, are very different.[80] The

https://doi.org/10.1557/mrc.2017.100 Published online by Cambridge University Press

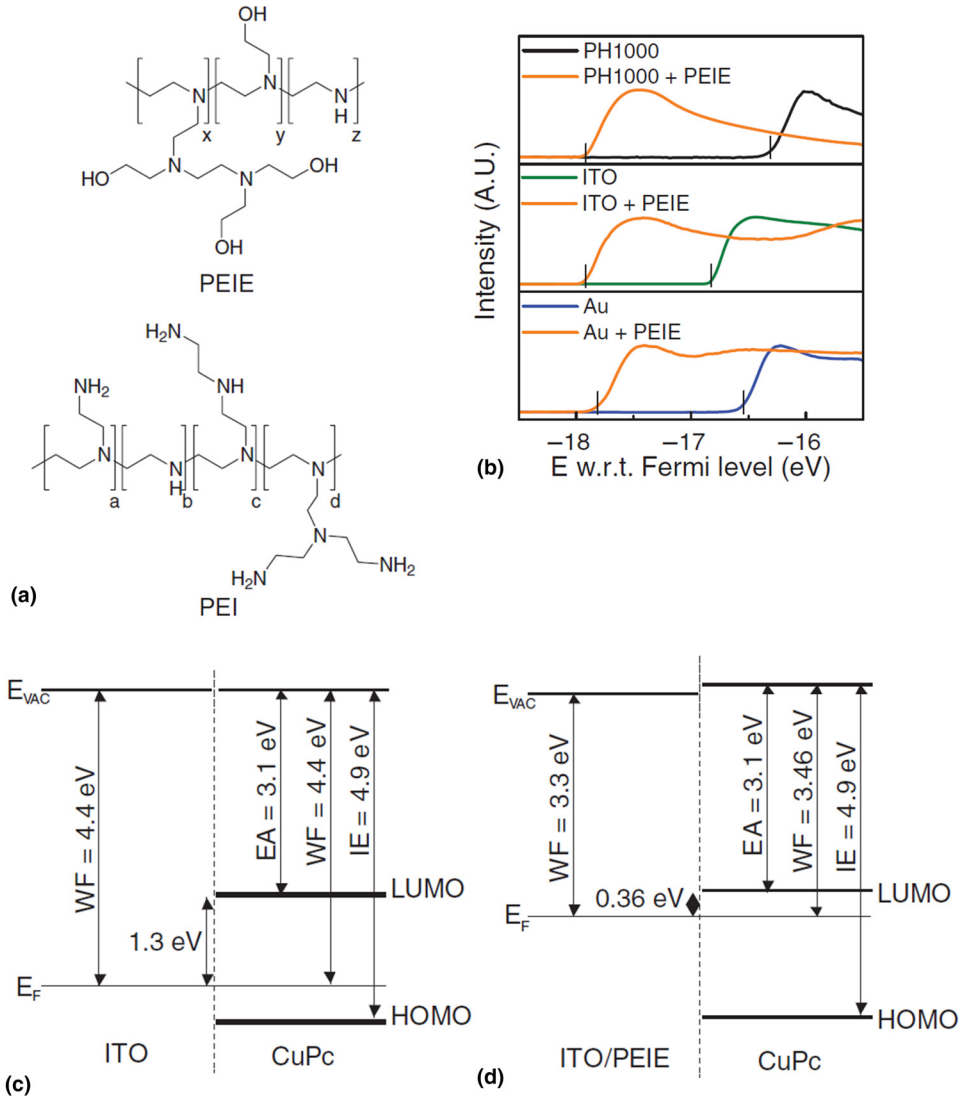


Figure 6. (a) Chemical structures of PEIE and PEI. (b) Ultraviolet photoemission spectroscopy measurements of PEIE deposited on PEDOT:PSS PH1000, ITO, and Au. Energy band diagrams of (c) ITO/CuPc, and (d) ITO/PEIE/CuPc structure, where E_{VAC} is the vacuum level positions, E_F is the Fermi level, WF is the work function, EA is the electron affinity, and IE is the ionization energy. Reproduced with permission from Ref. 86, Copyright 2012 AAAS.

grazing incidence XRD patterns showed that the CuPc film on the PEIE/Au surface exhibited edge-on orientation, while the film on a pristine Au surface exhibited a higher fraction of face-on orientation, which is better for charge transport in the vertical direction. Therefore, the former structure showed a lower RR of 1.8×10^4 and a forward current density of 3.0×10^{-3} A/cm^2, but the latter structure presented a higher RR of 6.7×10^7 and a forward current density of 20 A/cm^2 at 2 V.

For the fabrication of low-cost organic rectifiers, conjugated polymers are one of the most important candidate materials. Recently, the mobility of the polymer semiconductor has dramatically improved to above 10 cm^2/V/s.[89,90] This was accomplished on the basis of understanding of the molecular structure and orientation. Efficient intermolecular charge transfer occurs by a π–π stacking interaction. Thus, reducing the π–π stacking distance is one of the key aspects to achieving high mobility. High-mobility polymers have been reported in the TFT structures, where the edge-on orientation [Fig. 8(a)] is preferable to minimize the π–π stacking distance along the lateral direction. Insertion of a long side chain is also a common technique for polymer TFTs, in order to form highly ordered crystalline domains.[91,92] However, this technique is undesirable in terms of the vertical charge-transporting devices. To improve the vertical charge transport property, face-on or end-on orientations would be preferable, as shown in Figs. 8(b) and 8(c). Skrypnychuk et al. reported that the vertical conductivity of poly(3-hexylthiophene) (P3HT) could be improved by employing a graphene electrode.[93] They found that P3HT on a

https://doi.org/10.1557/mrc.2017.100 Published online by Cambridge University Press

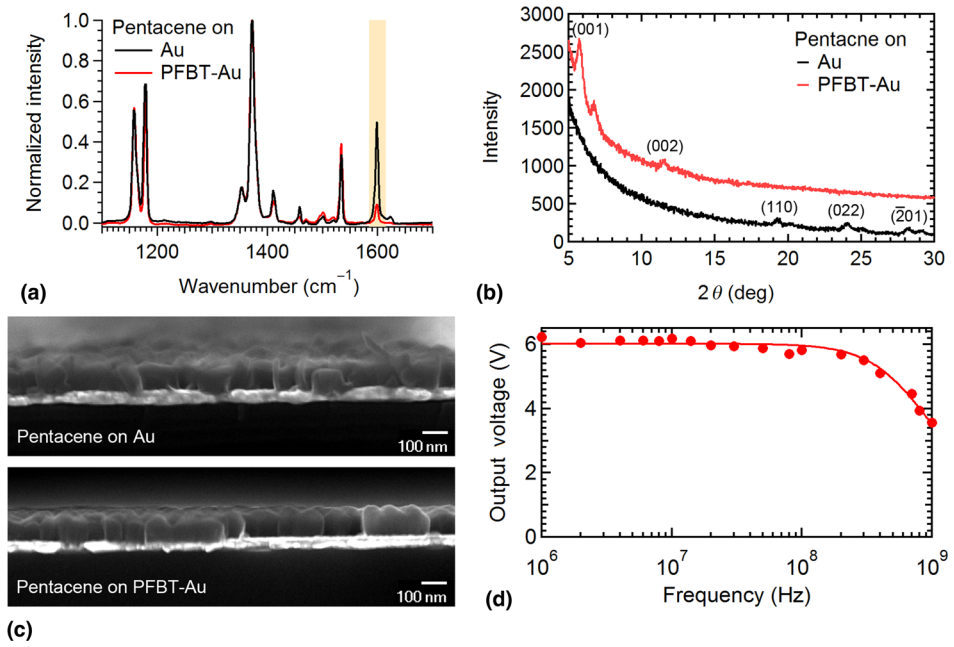


Figure 7. (a) Raman spectra and (b) XRD patterns of the pentacene films on PFBT-Au and Au. (c) Cross-sectional SEM images of pentacene films on PFBT-Au and Au. (d) Frequency response of the pentacene rectifier with PFBT-modified Au.

Si substrate predominantly had an edge-on orientation, whereas that on graphene exhibited a mixed edge-on and face-on orientations. The presence of face-on aggregates can create continuous pathways in the vertical direction, leading to improved vertical conductivity from 2.2×10^{-4} to 4.1×10^{-4} S/m. Another interesting method to improve the vertical charge transport is micro- or nanopatterning. Recent work showed that the vertical mobility of a spin-coated P3HT film was greatly enhanced after being imprinted with a micropatterned poly-dimethylsiloxane (PDMS) mold.[94] The formation of the micropillar structures partially changes the orientation of P3HT from edge-on to end-on, enabling efficient charge transport via delocalized electronic states of the conjugated polymer chain. Therefore, the vertical mobility of the micropatterned P3HT film was impressively increased from 10^{-4} to 3.1–10.6 cm^2/V/s. Even though the performance of the diode was not optimized in terms of charge injection efficiency and thickness, such a high vertical mobility presents a bright future for realizing gigahertz-operable polymer rectifiers.

Modifying the rectifying barrier height

The Schottky barrier formed at the metal/organic interface imparts rectifying characteristics to the diode. The reverse current of the diode is exponentially suppressed as the Schottky barrier height increases. Thus, the Schottky barrier height should be sufficient for HF organic rectifiers. A Schottky contact can be formed by mismatching between the HOMO or LUMO levels of the organic layer and the work function of the metal. For example, the HOMO level of polytriarylamine (PTAA) is known to 5.1 eV and forms an ohmic contact with high work function metals such as platinum (5.1–6.3 eV) and printed silver (5.2 eV), which leads to no rectifying characteristics for the PTAA diode.[59] However, a PTAA/copper electrode forms a rectifying contact, thereby reducing the reverse

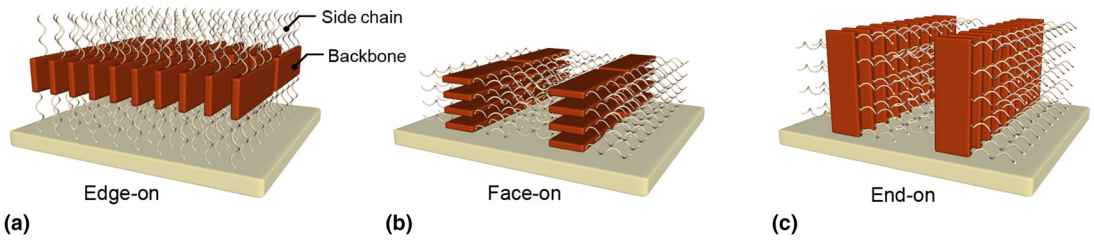


Figure 8. Orientation of the conjugated polymers: (a) edge-on, (b) face-on, and (c) end-on orientation.

https://doi.org/10.1557/mrc.2017.100 Published online by Cambridge University Press

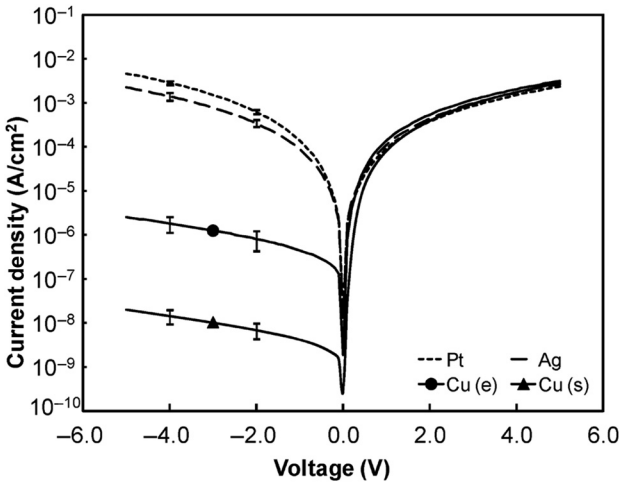


Figure 9. *J–V* characteristics of the PTAA diode with different cathodes. Reprinted with permission from Ref. 59, Copyright 2010 American Chemical Society.

current significantly by 3–5 orders of magnitude (Fig. 9). Interestingly, the leakage current depends not only on the selection of the metal, but also on the metal deposition method. The sputtered copper on PTAA additionally generated a thin insulating interfacial layer, preventing charge injection from copper to PTAA, which resulted in suppression of leakage current by two orders of magnitude compared with thermally evaporated copper.[59] The leakage current of the diode is an important issue in the rectifier because charge dissipation of the rectifier predominantly arises from the leakage current, which contributes to an additional output voltage drop.[12] In fact, the output voltage of the rectifier can be dropped more than expected because Joule heating by power consumption increases the temperature of the diode—the leakage current of the Schottky diode increases exponentially as a function of temperature due to thermionic emission. It has been reported that the leakage current of the organic Schottky diode increases approximately 100-fold when the temperature is increased from 300 to 400 K.[95] Thus, in terms of suppression of the leakage current, the barrier height of the organic diode should be high enough.

The barrier height also affects the forward current of the diode. Generally, the forward current of the organic Schottky diode is limited by either the contact or the bulk of semiconductor layer. The current is an exponential function of the voltage in the contact-limited regime [Eq. (5)] and a quadratic function of the voltage in the bulk-limited regime [Eq. (3)]. Therefore, the current predominantly obeys contact-limited in the low-voltage region and bulk-limited in the high-voltage region. If the mobility of the organic semiconductor is small, the transition voltage, where the dominant conduction mechanism changes from contact-limited to bulk-limited, is much lower so the forward current of the organic diode seems to be unchanged, even if the Schottky barrier height is changed [Figs. 9 and 10(a)].[59] However, if this transition occurs at a voltage higher than the operating voltage of the rectifier due to high mobility, the performance of the organic rectifier is greatly affected by the barrier height. In this case, sufficient charges can be supplied to the rectifier at a low voltage; thus, the operation voltage range for a charging period is much lower than in an organic rectifier with low mobility [Fig. 10(b)]. This indicates that the current characteristics in the low-voltage region play an important role in determining the frequency performance of the organic rectifier. Figure 11(a) shows the current density–voltage (*J–V*) characteristics of C_{60} diodes with interface layers of WO_3 and WO_3/hexamethyldisilazane (HMDS) for rectifying contacts. Due to the dipole moment of HMDS, the effective work function of WO_3/Al was shifted from 4.3 to 4.6 eV after the HMDS treatment. Compared with the forward current density of the C_{60} diode without the HMDS treatment, the forward current density of the C_{60}

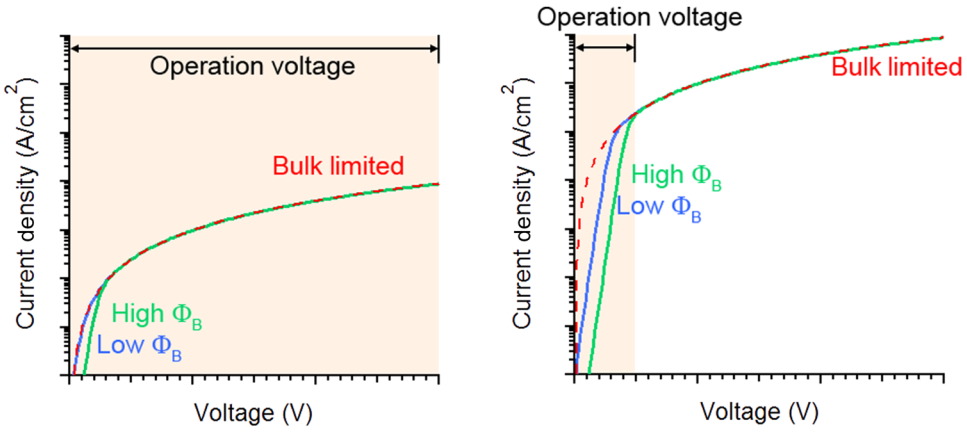


Figure 10. *J–V* characteristics of the organic diode with (a) low mobility and (b) high mobility as a function of Schottky barrier height (Φ_B). The shaded regions indicate the operation voltage region for the charging period of the organic rectifier.

https://doi.org/10.1557/mrc.2017.100 Published online by Cambridge University Press

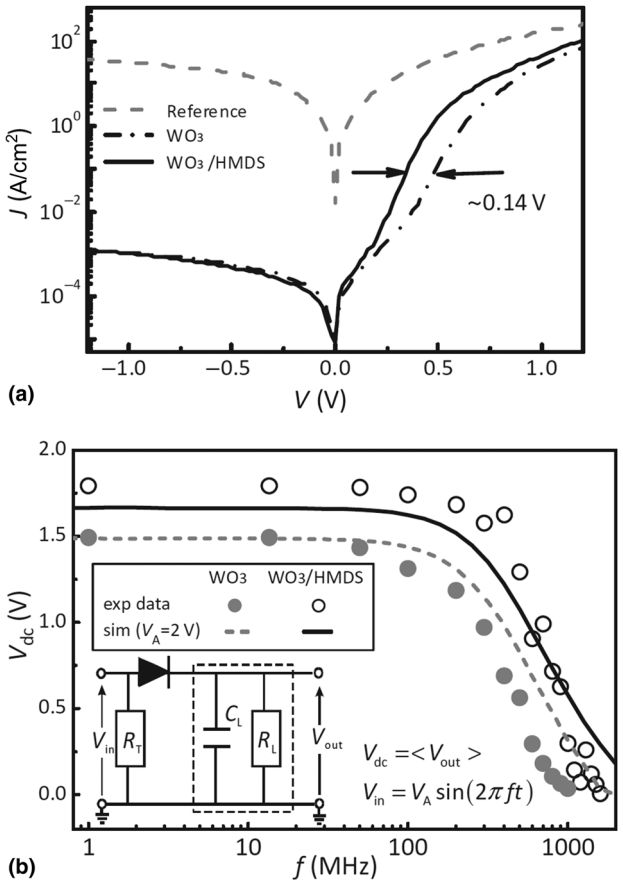


Figure 11. (a) *J–V* characteristics of the diodes comprising the Al/*X*/C_{60}/BCP/Al structure, where *X* is WO_3 (dash-dot), WO_3/HMDS (solid), or the absence of a layer (dash). (b) The average DC component (V_{dc}) of the output voltage (V_{out}) obtained for the 2 V sinusoidal incoming RF signal (V_{in}) with regard to the operating frequency for the C_{60} rectifiers with and without HMDS treatment. The shapes and lines indicate the experimental and the simulation results, respectively. The inset presents the rectifier circuit diagram for measurement, which consists of the C_{60} diode, 500 kΩ load resistor (R_L), 20 nF load capacitor (C_L), and 50 Ω resistor (R_T) for proper termination of the V_{in}. Reproduced with permission from Ref. 13, Copyright 2011 Wiley-VCH.

diode with the HMDS treatment was significantly improved below the 1-V range due to the decrease in barrier height. Moreover, the C_{60} rectifier with HMDS treatment showed only a 0.21 V output voltage drop and an improved 3 dB frequency of 700 MHz [Fig. 11(b)]. These results indicate that an excessively high barrier height would have detrimental effects on the performance of the high-speed organic diode. Therefore, the barrier height should be optimized to maximize the forward current, while the leakage current remains at an acceptable level.

Organic diode with pn-junction interface

For the pn-junction diode, high mobility of p-type and n-type semiconductors is a prerequisite for a HF rectifier. Unfortunately, the development of high mobility, air-stable n-type organic semiconductors has been lagging behind compared to p-type organic semiconductors because materials having high electron affinity are generally sensitive under ambient conditions. Moreover, stacking organic materials is also an issue for the low-cost solution process because the pre-deposited organic layer can be damaged or even washed out by an organic solvent while forming the upper organic layer. To overcome these issues, various p-type organic/n-type inorganic hybrid pn-junction diodes have been proposed.[36–39,60,96] Zinc oxide has widely been adopted as the n-type inorganic material for hybrid rectifiers because it possesses adequate mobility (>1 cm^2/V/s) and it can be solution processed, eco-friendly, and insoluble to organic solvents.[36–39,60,96] Previous reports have demonstrated pentacene/ZnO rectifiers with rectifying and switching characteristics.[36,38] A high-current density of 160 A/cm^2 at 5 V and a reverse breakdown voltage of 25 V were achieved and this allowed the operating frequency to reach more than 20 MHz.[36] For the solution processed p-type organic semiconductor, PEDOT:PSS, poly(3,3′-didodecylquaterthiophene) (PQT-12), and P3HT have been employed.[37,39,60,96] Since the charge carrier transport property of inorganic materials is superior to that of organic materials, a desirable design strategy of the hybrid diode is maximizing electron transport while the potential barrier at the organic/inorganic pn-junction properly gives the rectification behavior. Katsia et al. made a P3HT/ZnO diode with an electron barrier much lower than the hole barrier and, therefore, the electrons acted as a dominant current conduction source.[96] A remarkable forward current density of 10,000 A/cm^2 at 4 V with an RR of 10^5 was achieved.[96] Improvement of electrical characteristics through energy level shifting of the pn-junction potential using the SAM treatment has also been reported.[60] By employing the OTS (octadecyltrichlorosilane) treatment at the interface of ZnO/P3HT, the dipole-induced energy level shifted to lower the electron barrier, leading the hybrid pn-junction diode to achieve a 32-fold higher forward current and a 10-fold higher RR. In the case of using n-type organic materials for a pn-junction diode, C_{60} has been widely used, where the electron mobility can be similar to the hole mobility of p-type organic materials.[40,69,97] In this structure, the charge carriers are accumulated at the organic/organic interface as a consequence of the high electron and hole barriers. When the forward bias is applied, accumulated electrons and holes are non-radiatively recombined, resulting in a high forward current at low voltages. This was confirmed by fabricating hole-only and electron-only devices, where the forward current was greatly decreased compared with that for a diode, indicating that the charge injection at the organic/organic interface is almost prohibited.[97] When the reverse bias is applied, charge injection is limited by the injection barrier at the metal/organic interfaces. As a result, an N,N′-bis(naphthalen-1-yl)-N,N′-bis(phenyl)-benzidine (NPB)/C_{60} pn-junction diode showed a forward current density of 500 mA/cm^2 at 2.6 V and an RR of 7.8×10^4.[97] The device performance can be further improved by employing a p-doped/intrinsic/n-doped (PIN) diode

https://doi.org/10.1557/mrc.2017.100 Published online by Cambridge University Press

structure.[40] In this case, the metal/doped organic interfaces should form quasi-ohmic contacts, facilitating charge injection from metal to organic interfaces regardless of the metal work function. The current density and transit time of the PIN diode strongly depends on the doping concentration and thickness of the intrinsic organic layer. By optimizing the doping concentration (1 wt%) and the thickness of the intrinsic layer (90 nm), the p-doped pentacene/pentacene/n-doped C_{60} PIN rectifier showed an output voltage of 1.4 V at 20 MHz and even a voltage of 0.5 V at 300 MHz when an input voltage of 2 V was applied.[40]

Conclusions

High-frequency organic rectifiers require high forward current with low leakage current, turn-on voltage, and areal capacitance, and these can be achieved through interface engineering. The energy barrier formed at the interface can be controlled by dipole-induced energy level shift using chemical treatments or inserting a charge injection layer such as a conducting polymer, a doped organic layer, or a transition metal oxide for either high injection efficiency or rectification. Additionally, the molecular orientation and crystalline order of the organic layer can also be improved by modifying the surface properties of the bottom layer. By virtue of interface engineering, the operating frequency of the organic rectifiers has recently reached values in the GHz region, which is suitable for UHF use. However, issues such as a large output voltage drop at high frequency and stability under ambient conditions have been left unsettled to date. These issues are principally attributed to the poor mobility and instability of the organic semiconductors. However, the electrical properties and stability of organic semiconductors have rapidly been improving and will continue to be developed due to their unlimited molecular design tunability. Therefore, we are optimistic that practical use of UHF organic rectifiers will be achieved in the near future.

Acknowledgments

This work was supported by the Industrial Strategic Technology Development Program (10042537 and 10077471), ICT & R&D Voucher Program (2017-0-00836) supported by Ministry of Science, ICT and Future Planning, and the National Research Foundation of Korea (2016R1A2B3009301).

References

1. D. Voss: Cheap and cheerful circuits. *Nature* **407**, 442 (2000).
2. M. Berggren, D. Nilsson, and N.D. Robinson: Organic materials for printed electronics. *Nat. Mater.* **6**, 3 (2007).
3. J. Lee, W.J. Sung, C.W. Joo, H. Cho, N. Cho, G.W. Lee, D.H. Hwang, and J.I. Lee: Simplified bilayer white phosphorescent organic light-emitting diodes. *ETRI J.* **38**, 260 (2016).
4. S.W. Jung, B.S. Na, K.J. Baeg, M. Kim, S.M. Yoon, J. Kim, D.Y. Kim, and I.K. You: Nonvolatile ferroelectric P(VDF-TrFE) memory transistors based on inkjet-printed organic semiconductor. *ETRI J.* **35**, 734 (2013).
5. Y.H. Kim, D.G. Moon, and J.I. Han: Organic TFT array on a paper substrate. *IEEE Electron Device Lett.* **25**, 702 (2004).
6. S.R. Forrest: The path to ubiquitous and low-cost organic electronic appliances on plastic. *Nature* **428**, 911 (2004).
7. K. Myny, M. Rockelé, A. Chasin, D.V. Pham, J. Steiger, S. Botnaras, D. Weber, B. Herold, J. Ficker, B. Der Van Putten, G.H. Gelinck, J. Genoe, W. Dehaene, and P. Heremans: Bidirectional communication in an HF hybrid organic/solution-processed metal-oxide RFID tag. *IEEE Trans. Electron Devices* **61**, 2387 (2014).
8. M. Shakiba, A. Zavvari, N. Aleebrahim, and M.J. Singh: Evaluating the academic trend of RFID technology based on SCI and SSCI publications from 2001 to 2014. *Scientometrics* **109**, 591 (2016).
9. V. Fiore, P. Battiato, S. Abdinia, S. Jacobs, I. Chartier, R. Coppard, G. Klink, E. Cantatore, E. Ragonese, and G. Palmisano: An integrated 13.56-MHz RFID tag in a printed organic complementary TFT technology on flexible substrate. *IEEE Trans. Circuits Syst. I Regul. Pap.* **62**, 1668 (2015).
10. P.F. Baude, D.A. Ender, M.A. Haase, T.W. Kelley, D. V. Muyres, and S.D. Theiss: Pentacene-based radio-frequency identification circuitry. *Appl. Phys. Lett.* **82**, 3964 (2003).
11. K. Myny, S. Steudel, P. Vicca, M.J. Beenhakkers, N.A.J.M. van Aerle, G. H. Gelinck, J. Genoe, W. Dehaene, and P. Heremans: Plastic circuits and tags for 13.56 MHz radio-frequency communication. *Solid. State. Electron.* **53**, 1220 (2009).
12. C. Kang, J. Wade, S. Yun, J. Lim, H. Cho, J. Roh, H. Lee, S. Nam, D.D. C. Bradley, J.-S. Kim, and C. Lee: 1 GHz pentacene diode rectifiers enabled by controlled film deposition on SAM-treated au anodes. *Adv. Electron. Mater.* **2**, 1500282 (2016).
13. D. Im, H. Moon, M. Shin, J. Kim, and S. Yoo: Towards gigahertz operation: ultrafast low turn-on organic diodes and rectifiers based on C_{60} and tungsten oxide. *Adv. Mater.* **23**, 644 (2011).
14. S. Steudel, K. Myny, V. Arkhipov, C. Deibel, S. De Vusser, J. Genoe, and P. Heremans: 50 MHz rectifier based on an organic diode. *Nat. Mater.* **4**, 597 (2005).
15. Y. Ai, S. Gowrisanker, H. Jia, I. Trachtenberg, E. Vogel, R.M. Wallace, B.E. Gnade, R. Barnett, H. Stiegler, and H. Edwards: 14MHz organic diodes fabricated using photolithographic processes. *Appl. Phys. Lett.* **90**, 262105 (2007).
16. K. Myny, S. Steudel, P. Vicca, J. Genoe, and P. Heremans: An integrated double half-wave organic Schottky diode rectifier on foil operating at 13.56 MHz. *Appl. Phys. Lett.* **93**, 093305 (2008).
17. H. Wang, Z. Ji, L. Shang, X. Liu, Y. Peng, and M. Liu: Interface effect on the performance of rectifier based on organic diode. *IEEE Electron Device Lett.* **31**, 506 (2010).
18. C. Kang, Y. Hong, and C. Lee: Frequency performance optimization of flexible pentacene rectifier by varying the thickness of active layer. *Jpn. J. Appl. Phys.* **49**, 05EB07 (2010).
19. C. Kang, H. Cho, H. Lee, and C. Lee: Organic rectifier with transfer-printed metal as a top electrode. *J. Korean Phys. Soc.* **59**, 470 (2011).
20. N.V. Cvetkovic, K. Sidler, V. Savu, J. Brugger, D. Tsamados, and A. M. Ionescu: Organic half-wave rectifier fabricated by stencil lithography on flexible substrate. *Microelectron. Eng.* **100**, 47 (2012).
21. G. Gutierrez-Heredia, V.H. Martinez-Landeros, F.S. Aguirre-Tostado, P. Shah, B.E. Gnade, M. Sotelo-Lerma, and M.A. Quevedo-Lopez: Full bridge circuit based on pentacene schottky diodes fabricated on plastic substrates. *Semicond. Sci. Technol.* **27**, 85013 (2012).
22. Y. Ai, S. Gowrisanker, H. Jia, M. Quevedo-Lopez, H.N. Alshareef, R. M. Wallace, and B.E. Gnade: Encapsulation of high frequency organic Schottky diodes. *Thin Solid Films* **531**, 509 (2013).
23. C. Kang, H. Cho, M. Park, J. Roh, and C. Lee: Effects of insertion of hole injection layers on pentacene rectifying diodes. *J. Nanosci. Nanotechnol.* **14**, 5301 (2014).
24. S. Kim, H. Cho, Y. Hong, and C. Lee: Effect of electrode area on high speed characteristics over 1 MHz of poly(3-hexylthiophene-2,5-diyl) diode with Inkjet-printed Ag electrode. *Mol. Cryst. Liq. Cryst.* **513**, 256 (2009).
25. K.E. Lilja, T.G. Bäcklund, D. Lupo, T. Hassinen, and T. Joutsenoja: Gravure printed organic rectifying diodes operating at high frequencies. *Org. Electron.* **10**, 1011 (2009).
26. C. Kang, S. Kim, Y. Hong, and C. Lee: Frequency analysis on poly (3-hexylthiopene) rectifier using impedance spectroscopy. *Thin Solid Films* **518**, 889 (2009).

https://doi.org/10.1557/mrc.2017.100 Published online by Cambridge University Press

27. K. Kang Dae, K. Jae Bon, N. Yong-Young, L. Jong Keun, Y. Yong Suk, and Y. In-Kyu: Variations in the electric characteristics of an organic Schottky diode with the P3HT thickness. *J. Korean Phys. Soc.* **57**, 124 (2010).
28. C.-Y. Lin, C.-H. Tsai, H.-T. Lin, L.-C. Chang, Y.-H. Yeh, Z. Pei, Y.-R. Peng, and C.-C. Wu: High-frequency polymer diode rectifiers for flexible wireless power-transmission sheets. *Org. Electron.* **12**, 1777 (2011).
29. P.S. Heljo, M. Li, K.E. Lilja, H.S. Majumdar, and D. Lupo: Printed half-wave and full-wave rectifier circuits based on organic diodes. *IEEE Trans. Electron Devices* **60**, 870 (2013).
30. M. Li, P.S. Heljo, and D. Lupo: Organic rectifying diode and circuit for wireless power harvesting at 13.56 MHz. *IEEE Trans. Electron Devices* **61**, 2164 (2014).
31. S. Altazin, R. Clerc, R. Gwoziecki, J.-M. Verilhac, D. Boudinet, G. Pananakakis, G. Ghibaudo, I. Chartier, and R. Coppard: Physics of the frequency response of rectifying organic Schottky diodes. *J. Appl. Phys.* **115**, 064509 (2014).
32. I. Bose, K. Tetzner, K. Borner, and K. Bock: Air-stable, high current density, solution-processable, amorphous organic rectifying diodes (ORDs) for low-cost fabrication of flexible passive low frequency RFID tags. *Microelectron. Reliab.* **54**, 1643 (2014).
33. P. Heljo, K.E. Lilja, H.S. Majumdar, and D. Lupo: High rectifier output voltages with printed organic charge pump circuit. *Org. Electron.* **15**, 306 (2014).
34. P.S. Heljo, C. Schmidt, R. Klengel, H.S. Majumdar, and D. Lupo: Electrical and thermal analysis of frequency dependent filamentary switching in printed rectifying diodes. *Org. Electron.* **20**, 69 (2015).
35. J. Semple, S. Rossbauer, C.H. Burgess, K. Zhao, L.K. Jagadamma, A. Amassian, M.A. McLachlan, and T.D. Anthopoulos: Radio frequency coplanar ZnO Schottky nanodiodes processed from solution on plastic substrates. *Small* **12**, 1993 (2016).
36. B.N. Pal, J. Sun, B.J. Jung, E. Choi, A.G. Andreou, and H.E. Katz: Pentacene-zinc oxide vertical diode with compatible grains and 15-MHz rectification. *Adv. Mater.* **20**, 1023 (2008).
37. J. Sun, B.N. Pal, B.J. Jung, and H.E. Katz: Solution-processed hybrid p–n junction vertical diode. *Org. Electron.* **10**, 1 (2009).
38. K.H. Lee, A. Park, S. Im, Y. Park, S.H. Kim, M.M. Sung, and S. Lee: Advantageous reverse recovery behavior of pentacene/ZnO diode. *Electrochem. Solid-State Lett.* **13**, H261 (2010).
39. H. Liem, H.S. Choy, and K.C. Yung: A prerequisite to achieving high performance polymer/inorganic thin film diodes. *Solid State Commun.* **150**, 1725 (2010).
40. H. Kleemann, S. Schumann, U. Jörges, F. Ellinger, K. Leo, and B. Lüssem: Organic pin-diodes approaching ultra-high-frequencies. *Org. Electron.* **13**, 1114 (2012).
41. S. Ali, J. Bae, and C.H. Lee: Organic diode with high rectification ratio made of electrohydrodynamic printed organic layers. *Electron. Mater. Lett.* **12**, 270 (2016).
42. L.A. Majewski, C. Balocco, R. King, S. Whitelegg, and A.M. Song: Fast polymer nanorectifiers for inductively coupled RFID tags. *Mater. Sci. Eng. B* **147**, 289 (2008).
43. L.A. Majewski and A.M. Song: 20 megahertz operation of organic nanodiodes. *Phys. Status Solidi B, Basic Solid State Phys.* **253**, 1507 (2016).
44. S. Steudel, S. De Vusser, K. Myny, M. Lenes, J. Genoe, and P. Heremans: Comparison of organic diode structures regarding high-frequency rectification behavior in radio-frequency identification tags. *J. Appl. Phys.* **99**, 114519 (2006).
45. D.-H. Lee, J.-M. Kim, J. Lee, and Y. Kim: Improved organic rectifier using polymethyl-methacrylate-poly 4-vinylphenol double layer. *Micro Nano Lett.* **6**, 567 (2011).
46. M. Uno, Y. Kanaoka, B.-S. Cha, N. Isahaya, M. Sakai, H. Matsui, C. Mitsui, T. Okamoto, J. Takeya, T. Kato, M. Katayama, Y. Usami, and T. Yamakami: Short-channel solution-processed organic semiconductor transistors and their application in high-speed organic complementary circuits and organic rectifiers. *Adv. Electron. Mater.* **1**, 1500178 (2015).
47. M. Uno, B.-S. Cha, Y. Kanaoka, and J. Takeya: High-speed organic transistors with three-dimensional organic channels and organic rectifiers based on them operating above 20MHz. *Org. Electron.* **20**, 119 (2015).
48. A. Fischer, R. Scholz, K. Leo, and B. Lüssem: An all C_{60} vertical transistor for high frequency and high current density applications. *Appl. Phys. Lett.* **101**, 213303 (2012).
49. A. Chasin, M. Nag, A. Bhoolokam, K. Myny, S. Steudel, S. Schols, J. Genoe, G. Gielen, and P. Heremans: Gigahertz operation of a-IGZO schottky diodes. *IEEE Trans. Electron Devices* **60**, 3407 (2013).
50. N. Sani, M. Robertsson, P. Cooper, X. Wang, M. Svensson, P. Andersson Ersman, P. Norberg, M. Nilsson, D. Nilsson, X. Liu, H. Hesselbom, L. Akesso, M. Fahlman, X. Crispin, I. Engquist, M. Berggren, and G. Gustafsson: All-printed diode operating at 1.6 GHz. *Proc. Natl. Acad. Sci. U.S.A.* **111**, 11943 (2014).
51. J. Zhang, Y. Li, B. Zhang, H. Wang, Q. Xin, and A. Song: Flexible indium-gallium-zinc-oxide Schottky diode operating beyond 2.45 GHz. *Nat. Commun.* **6**, 7561 (2015).
52. J. Zhang, H. Wang, J. Wilson, X. Ma, J. Jin, and A. Song: Room temperature processed ultrahigh-frequency indium-gallium-zinc-oxide schottky diode. *IEEE Electron Device Lett.* **37**, 389 (2016).
53. W.-C. Chen, P.-C. Hsu, C.-W. Chien, K.-M. Chang, C.-J. Hsu, C.-H. Chang, W.-K. Lee, W.-F. Chou, H.-H. Hsieh, and C.-C. Wu: Room-temperature-processed flexible n-InGaZnO/p-Cu_2O heterojunction diodes and high-frequency diode rectifiers. *J. Phys. D: Appl. Phys.* **47**, 365101 (2014).
54. M.Y. Irshaid, C. Balocco, Y. Luo, P. Bao, C. Brox-Nilsen, and A.M. Song: Zinc-oxide-based planar nanodiodes operating at 50 MHz. *Appl. Phys. Lett.* **99**, 092101 (2011).
55. L. Diao, C.D. Frisbie, D.D. Schroepfer, and P. Paul Ruden: Electrical characterization of metal/pentacene contacts. *J. Appl. Phys.* **101**, 014510 (2007).
56. N. Koch, A. Kahn, J. Ghijsen, J.-J. Pireaux, J. Schwartz, R.L. Johnson, and A. Elschner: Conjugated organic molecules on metal versus polymer electrodes: demonstration of a key energy level alignment mechanism. *Appl. Phys. Lett.* **82**, 70 (2003).
57. H. Ishii, K. Sugiyama, E. Ito, and K. Seki: Energy level alignment and interfacial electronic structures at organic/metal and organic/organic interfaces. *Adv. Mater.* **11**, 605 (1999).
58. L. Ma, J. Ouyang, and Y. Yang: High-speed and high-current density C_{60} diodes. *Appl. Phys. Lett.* **84**, 4786 (2004).
59. K.E. Lilja, H.S. Majumdar, F.S. Pettersson, R. Österbacka, and T. Joutsenoja: Enhanced performance of printed organic diodes using a thin interfacial barrier layer. *ACS Appl. Mater. Interfaces* **3**, 7 (2011).
60. R.K. Pandey, R. Mishra, P. Tiwari, and R. Prakash: Interface engineering for enhancement in performance of organic/inorganic hybrid heterojunction diode. *Org. Electron.* **45**, 26 (2017).
61. Y. Don Park, J.A. Lim, H.S. Lee, and K. Cho: Interface engineering in organic transistors. *Mater. Today* **10**, 46 (2007).
62. C. Di, Y. Liu, G. Yu, D. Zhu, D.Z.C. Di, Y. Liu, G. Yu, C. Di, Y. Liu, G. Yu, and D. Zhu: Interface engineering: an effective approach toward high-performance organic field-effect transistors. *Acc. Chem. Res.* **42**, 1573 (2009).
63. C. Liu, Y. Xu, and Y.Y. Noh: Contact engineering in organic field-effect transistors. *Mater. Today* **18**, 79 (2015).
64. H. Ishii, N. Hayashi, E. Ito, Y. Washizu, K. Sugi, Y. Kimura, M. Niwano, Y. Ouchi, and K. Seki: Kelvin probe study of band bending at organic semiconductor/metal interfaces: examination of Fermi level alignment. *Phys. Status Solidi* **201**, 1075 (2004).
65. S.K. Cheung and N.W. Cheung: Extraction of Schottky diode parameters from forward current–voltage characteristics. *Appl. Phys. Lett.* **49**, 85 (1986).
66. V. Mikhelashvili, G. Eisenstein, and R. Uzdin: Extraction of Schottky diode parameters with a bias dependent barrier height. *Solid State Electron.* **45**, 143 (2001).
67. J. Sworakowski and K. Pigoń: Trap distribution and space-charge limited currents in organic crystals. *J. Phys. Chem. Solids* **30**, 491 (1969).
68. P. de Bruyn, A.H.P. van Rest, G.A.H. Wetzelaer, D.M. de Leeuw, and P.W. M. Blom: Diffusion-limited current in organic metal-insulator-metal diodes. *Phys. Rev. Lett.* **111**, 186801 (2013).
69. H. Kleemann, R. Gutierrez, S. Avdoshenko, G. Cuniberti, K. Leo, and B. Lüssem: Reverse breakdown behavior in organic pin-diodes comprising C_{60} and pentacene: experiment and theory. *Org. Electron.* **14**, 193 (2013).

https://doi.org/10.1557/mrc.2017.100 Published online by Cambridge University Press

70. M.Y. Chan, S.L. Lai, M.K. Fung, S.W. Tong, C.S. Lee, and S.T. Lee: Efficient CsF/Yb/Ag cathodes for organic light-emitting devices. *Appl. Phys. Lett.* **82**, 1784 (2003).
71. I.H. Campbell, S. Rubin, T.A. Zawodzinski, J.D. Kress, R.L. Martin, D.L. Smith, N.N. Barashkov, and J.P. Ferraris: Controlling Schottky energy barriers in organic electronic devices using self-assembled monolayers. *Phys. Rev. B* **54**, R14321 (1996).
72. I.H. Campbell, J.D. Kress, R.L. Martin, D.L. Smith, N.N. Barashkov, and J. P. Ferraris: Controlling charge injection in organic electronic devices using self-assembled monolayers. *Appl. Phys. Lett.* **71**, 3528 (1997).
73. J. Kwon, Y.G. Seol, N.-E. Lee, and I. Chung: Study on Ohmic contact improvement of organic Schottky diode utilizing self-assembled monolayer and PEDOT:PSS layers. *J. Vac. Sci. Technol. A* **28**, 879 (2010).
74. N. Koch, A. Elschner, J. Schwartz, and A. Kahn: Organic molecular films on gold versus conducting polymer: influence of injection barrier height and morphology on current–voltage characteristics. *Appl. Phys. Lett.* **82**, 2281 (2003).
75. G. Heywang and F. Jonas: Poly(alkylenedioxythiophene)s—new, very stable conducting polymers. *Adv. Mater.* **4**, 116 (1992).
76. J. Kido and T. Matsumoto: Bright organic electroluminescent devices having a metal-doped electron-injecting layer. *Appl. Phys. Lett.* **73**, 2866 (1998).
77. X. Zhou, M. Pfeiffer, J. Blochwitz, A. Werner, A. Nollau, T. Fritz, and K. Leo: Very-low-operating-voltage organic light-emitting diodes using a p-doped amorphous hole injection layer. *Appl. Phys. Lett.* **78**, 410 (2001).
78. S.-F. Chen and C.-W. Wang: Influence of the hole injection layer on the luminescent performance of organic light-emitting diodes. *Appl. Phys. Lett.* **85**, 765 (2004).
79. S. Tokito, K. Noda, and Y. Taga: Metal oxides as a hole-injecting layer for an organic electroluminescent device. *J. Phys. D, Appl. Phys.* **29**, 2750 (1996).
80. N. Matsuhisa, H. Sakamoto, T. Yokota, P. Zalar, A. Reuveny, S. Lee, and T. Someya: A mechanically durable and flexible organic rectifying diode with a polyethylenimine ethoxylated cathode. *Adv. Electron. Mater.* **2**, 1600259 (2016).
81. M.A. Mezour, O. Voznyy, E.H. Sargent, R.B. Lennox, and D.F. Perepichka: Controlling C_{60} organization through dipole-induced band alignment at self-assembled monolayer interfaces. *Chem. Mater.* **28**, 8322 (2016).
82. M. Kröger, S. Hamwi, J. Meyer, T. Riedl, W. Kowalsky, and A. Kahn: Role of the deep-lying electronic states of MoO_3 in the enhancement of hole-injection in organic thin films. *Appl. Phys. Lett.* **95**, 123301 (2009).
83. H.Y. Yu, X.D. Feng, D. Grozea, Z.H. Lu, R.N.S. Sodhi, A.-M. Hor, and H. Aziz: Surface electronic structure of plasma-treated indium tin oxides. *Appl. Phys. Lett.* **78**, 2595 (2001).
84. Y. Ueda, J. Abe, H. Murata, Y. Gotoh, and O. Sakai: Control of work function of indium tin oxide: A surface treatment by atmospheric-pressure plasma layer on fabric-type electrodes. *Jpn. J. Appl. Phys.* **53**, 03DG03 (2014).
85. Z. Jia, V.W. Lee, I. Kymissis, L. Floreano, A. Verdini, A. Cossaro, and A. Morgante: In situ study of pentacene interaction with archetypal hybrid contacts: Fluorinated versus alkane thiols on gold. *Phys. Rev. B* **82**, 125457 (2010).
86. Y. Zhou, C. Fuentes-Hernandez, J. Shim, J. Meyer, A.J. Giordano, H. Li, P. Winget, T. Papadopoulos, H. Cheun, J. Kim, M. Fenoll, A. Dindar, W. Haske, E. Najafabadi, T.M. Khan, H. Sojoudi, S. Barlow, S. Graham, J.-L. Bredas, S.R. Marder, A. Kahn, and B. Kippelen: A universal method to produce low-work function electrodes for organic electronics. *Science* **336**, 327 (2012).
87. D. Käfer, L. Ruppel, and G. Witte: Growth of pentacene on clean and modified gold surfaces. *Phys. Rev. B* **75**, 085309 (2007).
88. W.S. Hu, Y.T. Tao, Y.J. Hsu, D.H. Wei, and Y.S. Wu: Molecular orientation of evaporated pentacene films on gold: Alignment effect of self-assembled monolayer. *Langmuir* **21**, 2260 (2005).
89. G. Kim, S.-J. Kang, G.K. Dutta, Y.-K. Han, T.J. Shin, Y.-Y. Noh, and C. Yang: A thienoisoindigo-naphthalene polymer with ultrahigh mobility of 14.4 $cm^2/V{\cdot}s$ that substantially exceeds benchmark values for amorphous silicon semiconductors. *J. Am. Chem. Soc.* **136**, 9477 (2014).
90. C. Luo, K.K. Kyaw, L.A. Perez, S. Patel, M. Wang, B. Grimm, G.C. Bazan, E.J. Kramer, and A.J. Heeger: General strategy for self-assembly of highly oriented nanocrystalline semiconducting polymers with high mobility. *Nano Lett.* **14**, 2764 (2014).
91. I. Kang, H.J. Yun, D.S. Chung, S.K. Kwon, and Y.H. Kim: Record high hole mobility in polymer semiconductors via side-chain engineering. *J. Am. Chem. Soc.* **135**, 14896 (2013).
92. J. Lee, A.R. Han, H. Yu, T.J. Shin, C. Yang, and J.H. Oh: Boosting the ambipolar performance of solution-processable polymer semiconductors via hybrid side-chain engineering. *J. Am. Chem. Soc.* **135**, 9540 (2013).
93. V. Skrypnychuk, N. Boulanger, V. Yu, M. Hilke, S.C.B. Mannsfeld, M. F. Toney, and D.R. Barbero: Enhanced vertical charge transport in a semiconducting p3ht thin film on single layer graphene. *Adv. Funct. Mater.* **25**, 664 (2015).
94. V. Skrypnychuk, G.J.A.H. Wetzelaer, P.I. Gordiichuk, S.C.B. Mannsfeld, A. Herrmann, M.F. Toney, and D.R. Barbero: Ultrahigh Mobility in an Organic Semiconductor by Vertical Chain Alignment. *Adv. Mater.* **28**, 2359 (2016).
95. A.A.M. Farag and I.S. Yahia: Rectification and barrier height inhomogeneous in Rhodamine B based organic Schottky diode. *Synth. Met.* **161**, 32 (2011).
96. E. Katsia, N. Huby, G. Tallarida, B. Kutrzeba-Kotowska, M. Perego, S. Ferrari, F.C. Krebs, E. Guziewicz, M. Godlewski, V. Osinniy, and G. Luka: Poly(3-hexylthiophene)/ZnO hybrid pn junctions for microelectronics applications. *Appl. Phys. Lett.* **94**, 143501 (2009).
97. S.J. He, R. White, D.K. Wang, J. Zhang, N. Jiang, and Z.H. Lu: A simple organic diode structure with strong rectifying characteristics. *Org. Electron.* **15**, 3370 (2014).

https://doi.org/10.1557/mrc.2017.100 Published online by Cambridge University Press